Ocean Engineering 161 (2018) 69–76

Contents lists available at ScienceDirect

Ocean Engineering

journal homepage: www.elsevier.com/locate/oceaneng

Classification of vessel motion pattern in inland waterways based on Automatic Identification System

Zhijun Chen [a,b], Jie Xue [a,b], Chaozhong Wu [a,b,*], LingQiao Qin [c], Liqun Liu [a,b], Xiaozhao Cheng [a,b]

[a] National Engineering Research Center for Water Transport Safety, Wuhan University of Technology, Wuhan, 430063, China
[b] Intelligent Transport Systems Research Center, Wuhan University of Technology, Wuhan, 430063, China
[c] Department of Civil and Environment Engineering, University of Wisconsin-Madison, Madison, WI, USA

ARTICLE INFO

Keywords:
Waterway transportation
Classification model
Vessel motion pattern
Sparse reconstruction
Automatic Identification System

ABSTRACT

With the development of terrestrial networks and satellite constellations, vessel movement information can be effectively collected based on Automatic Identification System (AIS) receivers. Vessel motion pattern classification using AIS plays an important role in maritime monitoring and management. However, classifying vast amounts of vessel motion information is prohibitive workload. The aim of this study is to develop effective methods that can aid in automatic vessel motion pattern classification in inland waterways. First, the Least-squares Cubic Spline Curves Approximation (LCSCA) technique is used to represent the vessel motion trajectory. Then, a traditional classification model based on Lp-norm ($0 < p < 1$) sparse representation is improved to classify vessel motion patterns. And a Matching Pursuit - Fletcher Reeves (MPFR) method is developed to find the sparse solutions of the proposed model. To validate the performance of the proposed model, two AIS datasets from the Yangtze River are collected and applied in our experiment. According to the results, we can know that the proposed model can effectively classify vessel motion pattern in inland waterways. And the effectiveness of the proposed model is superior to those of other representative classification methods.

1. Introduction

The Automatic Identification System (AIS) data can be divided into three different types (International Maritime Organization, 2003): static data, dynamic data and voyage-related data. Vessel information such as vessel name, type, speed, position and heading can be obtained from AIS. In recent years, advancement in electronic tracking techniques, remote sensing techniques and communication techniques has enabled the development and application AIS. In addition, legislations are now mandatory to have AIS equipment on board of international voyaging ships with 300 or more gross tonnage and cargo ships of 500 gross tons for the Safety of Life at Sea (SOLAS). In China, inland waterways ships are required to install AIS by the Maritime Safety Administration (MSA). Therefore, due to these legislations and the development of sensor technology, AIS has been widely applied in the maritime monitoring and management.

Classifying vessel motion patterns is one of the most important aspects of analyzing the AIS data, and it is useful for enhancing maritime monitoring, ship safety, and management technology. For instance, ship accidents may be avoided if the maritime authority can understand and warn against making dangerous ship movements, according to historical movements of vessels that had the same class of motion pattern. Therefore, many researchers are increasingly starting to pay attention to analyzing AIS data.

As mentioned above, AIS can provide many kinds of vessel information. In addition, more and more vessels are applied in inland waterways in China due to low price and good policy. Thus, vast amounts of AIS dataset are collected. However, the manual analysis of such large volumes of data involves a prohibitively large workload. According to the needs of many practical applications, extensive scholars focus on the classification model to identify object (e.g. vehicle) moving patterns. However, few studies pay attention to classify vessel motion patterns. Therefore, it is imperative to develop an effective method that can aid in the automatic classification of vessel motion patterns using AIS data for improving maritime management techniques and safety awareness. In China, although inland waterways transportation is fast developing, the transportation management develops slowly. In order to improve vessel monitoring and management in inland waterways, we only focus on inland waterways in this study.

An object motion characterization can be described using motion

* Corresponding author. National Engineering Research Center for Water Transport Safety, Wuhan University of Technology, Wuhan, 430063, China.
E-mail addresses: chenzj556@whut.edu.cn (Z. Chen), wucz@whut.edu.cn (C. Wu), xiaozhaocc@whut.edu.cn (X. Cheng).

https://doi.org/10.1016/j.oceaneng.2018.04.072
Received 1 September 2017; Received in revised form 18 April 2018; Accepted 18 April 2018
Available online 8 May 2018
0029-8018/

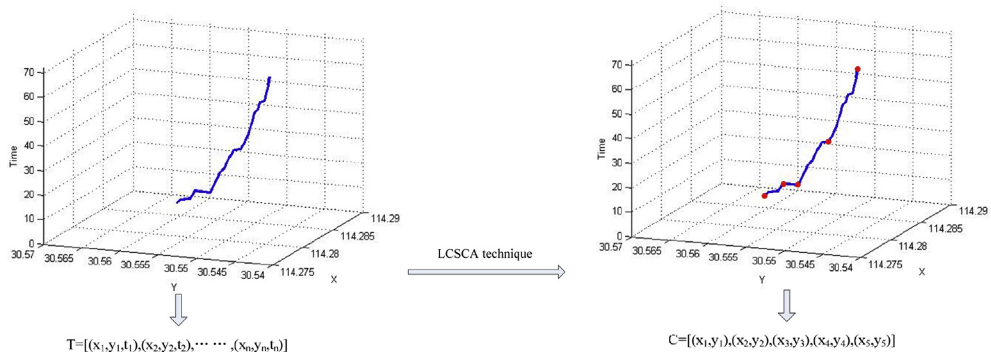

Fig. 1. Example of vessel trajectory representation with LCSCA (control points = 5).

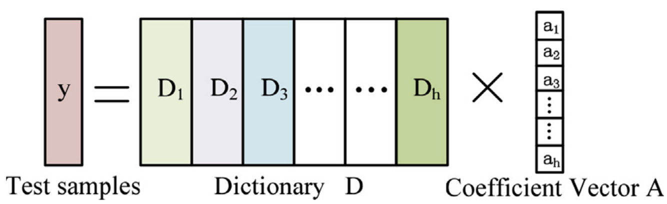

Fig. 2. Example of the data sample represented by a dictionary based on sparse representation.

trajectory that contain a sequence of position points. The motion trajectory has been widely employed to identify object motion patterns, action recognition, and so on (Bennewitz, 2005; Calinon et al., 2007; Moldenhauer et al., 2006; Psarrou et al., 2002; Yang et al., 2002; Hu et al., 2013). Thus, motion trajectories play an important role in the classification of moving patterns. For example, Schuldt et al. (Calinon et al., 2007) use motion trajectories to represent human action such as walking, jogging, and hand clapping. And a radial basis support vector machine (SVM) is employed to classify human actions (Yang et al., 2002).

A motion trajectory is used to describe the gesture motion, and gesture motion pattern can be classified using SVM model (Yu and Barner, 2008). Based on motion trajectory, Liao et al. (2007) propose a classification model using hierarchically structured conditional random fields to identify human motion patterns. Sun et al. (2015) propose a classification model to identify human motion patterns using beta process hidden Markov models (BP-HMM) based on human motion trajectories. Shao and Li (Cheng et al., 2016) propose two representation methods that are fingerlets for static gesture representations and strokelets for trajectory gesture representations. Based on two representation methods, Image-to-Class Dynamic Time Warping (I2C-DTW) method is proposed to classify hand gestures. Based on motion trajectory, a Dynamic Bayesian Network (DBN) model is used by Santos et al. (2015) to classify human action. In order to improve the performance and effectiveness of the model, a sliding window approach is applied. Fielda et al. (Field et al., 2015) use motion trajectory to describe human motions. Then an unsupervised classification method is developed based on a dynamic time alignment of Gaussian mixture model clusters. Using human motion trajectories, Chen et al. (2011) propose cluster method to classify human motion patterns. In this method, the long-term future motion can be also predicted.

Although the object motion patterns can be classified based on motion trajectory and learning methods, a large number of training trajectory is needed to training the model. For AIS dataset, labeling vessel motion patterns is a large workload by manually. In addition, the AIS dataset is often missing or incomplete. Thus, it is difficult to obtain sufficient training samples from AIS dataset. These learning methods introduced above may not achieve satisfactory performance.

The sparse representation classification (SRC) method is a novel idea in the field of classification. A good performance using SRC can

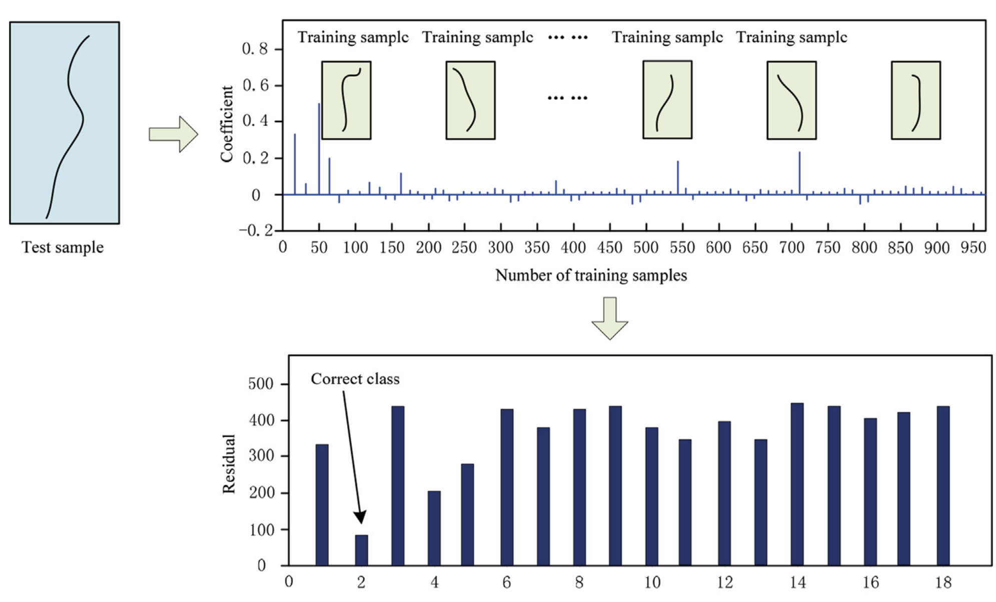

Fig. 3. An example illustration of vessel trajectory classification using SRC.

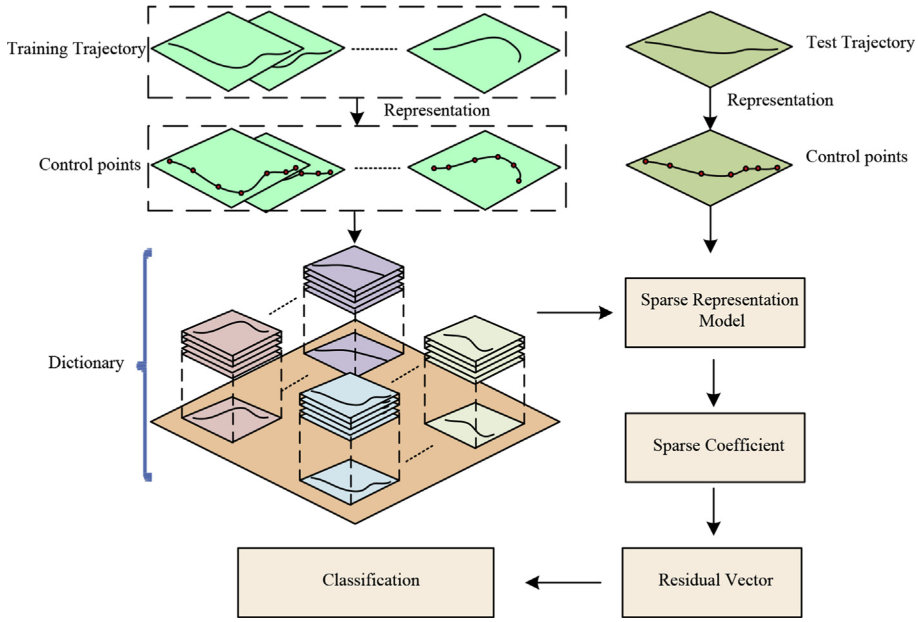

Fig. 4. The framework of the proposed method.

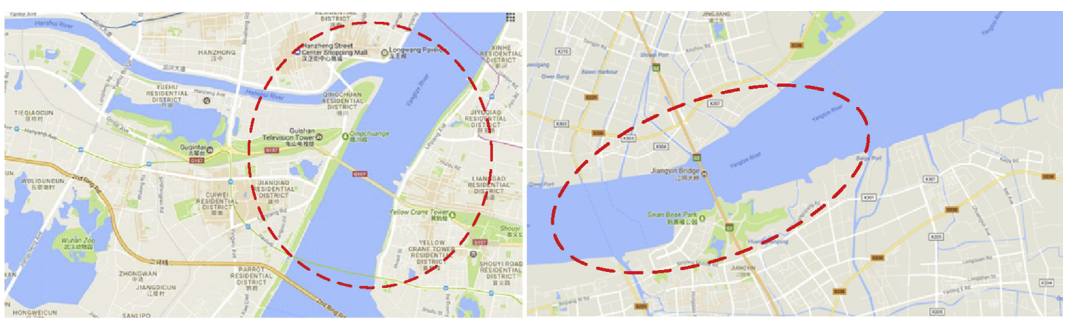

Fig. 5. The researched area and sensor device: (a)Wuhan, (b)Taizhou.

be achieved even if the features of training samples are insufficient or incomplete. The core problem of SRC is solve the L0-minimization, which is considered as an NP-hard problem (Amaldi and Kann, 1998). To this end, many studies change L0-minimization problems into L1-minimization ones. Thus, many convex optimization solvers (e.g., the second-order core programming solver) can be used to solve the sparse representation models within polynomial time. For example, the SRC based on L1-minimization is firstly used to identify human faces by Wright et al. (2009). Li et al. (2011) use the SRC method to classify motion pattern. In this study, a dictionary of SRC is generated using the trajectories expected from video surveillance. Based on convex optimization solvers, the sparse coefficients can be obtained. According to the dictionary and sparse coefficients, object motion pattern can be classified. Similarly, in another study by Ahmadi et al. (2016), SRC model based on L1-minimization is developed to classify vehicle motion patterns. However, the performance of SRC with L1-minimization cannot achieve satisfactory performance because the sparsity of solutions from L1-minimization is affected from the values of the entries in the norm. To this end, some researchers propose the SRC model with an Lp-minimization ($0 < p < 1$) to find sparser solutions. The problem of Lp-minimization is not convex. Thus the convex optimization solvers cannot be used to solve the sparse representation models. In order to address this problem, some studies prove that the local optimal solution of Lp-minimization can replace the global optimal solutions of L1-minimization (Chartrand, 2007a, 2007b; Fan and Li, 2001; Nikolova, 2005). The optimization solutions can be obtained even if the global optimal solutions cannot be found. For instance, Chen et al. (2017) propose a hybrid algorithm, where a quasi-Newton orthogonal matching pursuit approach is proposed to effectively find the sparse solutions of sparse representation models based on Lp-minimization.

In this study, a SRC model based on the Lp- minimization is proposed to classify vessel motion patterns. The distance between the test samples and the training samples is used to improve the sparse representation classification model. To solve the proposed model, a novel method, Matching Pursuit - Fletcher Reeves (MPFR), is developed in this study. To validate the performance of the proposed method, two AIS datasets from the Yangtze River are used in our experiment. The results show that the classification accuracies of the proposed method are superior to those of other representative classification methods, including Naive Bayes Classification (NBC), Support Vector Machine (SVM), k-Nearest Neighbor (kNN), and sparse reconstruction classification with Lp-norm (SRC-Lp), L1-norm (SRC-L1), and L2-norm (SRC-L2). The main contributions of this study are as follows:

(1) The improved sparse reconstruction classification model is developed to classify vessel motion patterns in inland waterways.
(2) A novel method, Matching Pursuit - Fletcher Reeves (MPFR), is proposed to solve the proposed sparse reconstruction classification model.

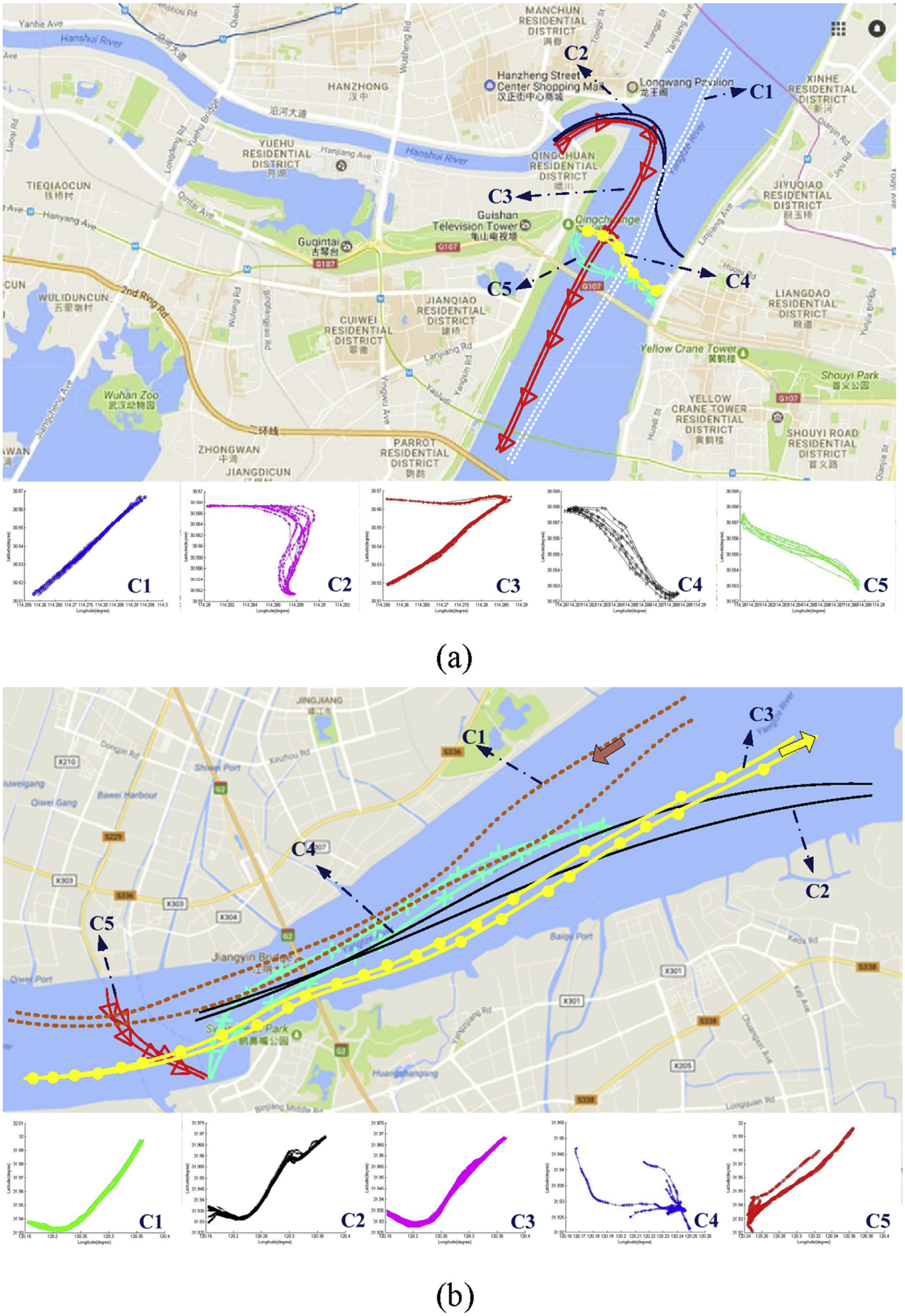

Fig. 6. The vessel motion patterns of sailing in the Yangtze River: (a)Wuhan, (b)Taizhou.

Table 1
General information of dataset used in our experiments.

Class	Wuhan dataset		Taizhou dataset	
	Training number	Test number	Training number	Test number
C1	555	200	355	350
C2	675	300	265	230
C3	730	260	387	300
C4	670	200	517	280
C5	830	350	233	290

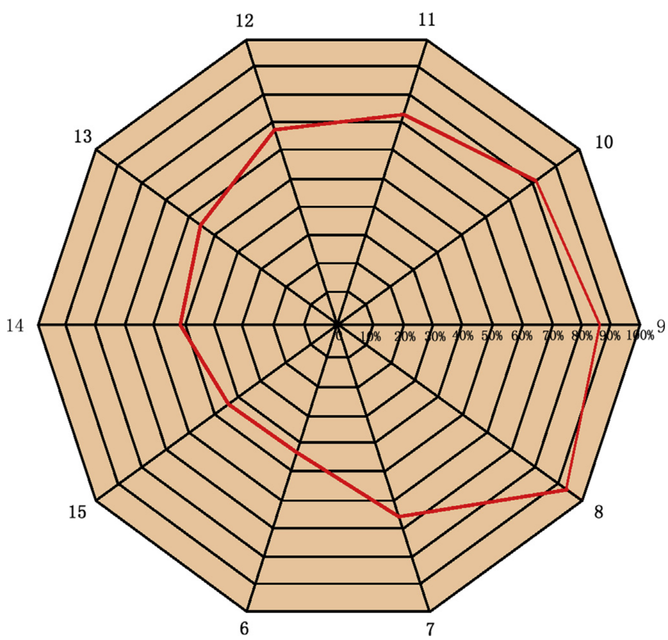

Fig. 7. The classification accuracy of the proposed method under different control points.

Table 2
Classification accuracy rate of vessel motion pattern using six methods under Wuhan dataset.

TPR	SVM	kNN	SRC-L1	SRC-L2	SRC-Lp	Our method
C1	86.5%	88%	88.5%	87%	89%	91%
C2	86.7%	88.3%	89.3%	88.7%	90.3%	91.6%
C3	84.6%	85.3%	88.1%	88.8%	89.6%	91.9%
C4	87%	87.5%	89%	86%	88.5%	90.5%
C5	85.4%	86.2%	88.9%	86.6%	89.4%	90.8%
Average	86%	87.1%	88.8%	87.4%	89.3%	91.2%

The rest of this study is structured as follows. In Section 2, the methodology used in this paper is introduced. The experimental dataset and results are described and analyzed in Section 3. Finally, we present the conclusion and discuss future work in Section 4.

2. Methodology

2.1. Trajectory representation

The motion trajectory, which can describe a sequence of moving positions of a tracked object, plays an important role in the field of moving patterns classification. Therefore, motion trajectories are applied to classify vessel motion patterns in this study. Since the motion trajectories of vessels collected by AIS are of different lengths, they cannot be directly used in SRC. To obtain fixed-length vectors of motion trajec-

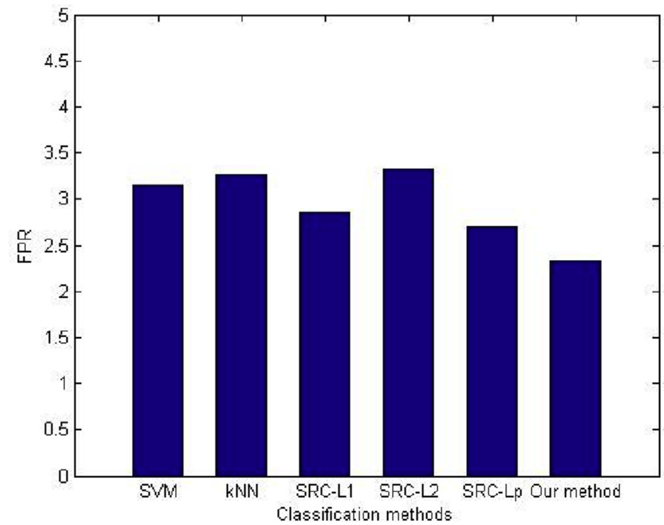

Fig. 8. The average FPR of classification vessel motion pattern using six methods under Wuhan dataset.

Table 3
Classification accuracy rate of vessel motion pattern using six methods under Taizhou dataset.

TPR	SVM	kNN	SRC-l1	SRC-L2	SRC-Lp	Our method
C1	85.7%	86.2%	88.6%	85.5%	89.1%	91.1%
C2	81.7%	80.8%	83.5%	86%	85.2%	88.2%
C3	83.7%	86%	87.3%	86.7%	89.7%	90.3%
C4	82.1%	82.9%	85.3%	85%	85.3%	86.8%
C5	86.2%	87.2%	89.3%	87.9%	91.3%	92.8%
Average	83.9%	84.6%	86.8%	86.2%	88.1%	89.8%

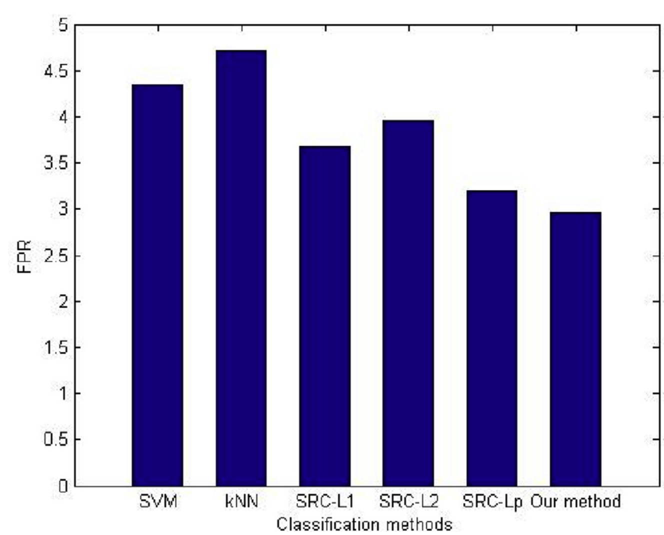

Fig. 9. The average FPR of classification vessel motion pattern using six methods under Taizhou dataset.

tories, the Least-squares Cubic Spline Curves Approximation (LCSCA) technique is employed (Sillito and Fisher, 2010). In this method, due to the complexity of the shape of curves can be described by spline curves, each motion trajectory can be approximated using a uniform cubic B-spline curve. A curve often can be generated by a sequence of points which are called control points. In this study, given a vessel trajectory sequence in (x, y, t) space, B-spline control points can be used to represent both the shape and spatio-temporal profiles of a trajectory,

$T^{XY} = \{T_1, T_2, \cdots T_n\} = \{(x_1, y_1, t_1), (x_2, y_2, t_2), \cdots (x_n, y_n, t_n)\}$, in the form of a parametric vector $C^{XY} = \{C_1^X, C_2^X, C_3^X, \cdots C_p^X, C_1^Y, C_2^Y, C_3^Y, \cdots C_p^Y\}$, where p is the number of control points, n is the length of trajectory, C_p^X is the represented x coordinate of the pth control point, and C_p^Y is the represented y coordinate of the pth control point. The detail of LCSCA technique can be found Appendix A. Fig. 1 shows a vessel trajectory being normalized by the LCSCA technique.

2.2. The proposed classification model

According to the SRC technique, any new test sample can be approximated using a linear combination of training samples. In this study, the sample is the vessel trajectory, and each training trajectory can be described as a vector d ($d \in R^m$) based on LCSCA. If there are h classes in the entire training set, the dictionary D of SRC can be described as follows:

$$D = [D_1, D_2, \cdots D_h,] = [d_{1,1}, \cdots d_{1,n}, \cdots d_{h,1}, \cdots d_{h,n}] \in R^{m \times n} \tag{1}$$

where $D_i = [d_{i,1}, \cdots d_{i,n}] (1 < i < h)$ is a sub-set of the training samples from class i and n is the number of the samples in class i. According to the theory of sparse representation, all of the test samples $Y = [y_1, y_2, \cdots y_\eta]$ can be represented by the dictionary D as

$$y = DA$$

where A is the representation coefficient vector of y on D, $y = [t_1, t_2, \cdots t_n]$. Fig. 2 shows an example of a data sample represented by a dictionary based on sparse representation (see Fig. 2).

To find A, the following model can be used:

$$\widehat{A} = \text{argmin}\{||y - DA||_2^2 + \lambda||A||_0\} \tag{2}$$

where A_0 is the l_0-norm of A.

According to the residuals and the corresponding training sample in the dictionary, the class of test sample can be identified as follow:

$$R = ||y - DA||_2$$

$$Classification(y) = arg\min_i (R_i) \quad i \in (1, 2, 3 \cdots h) \tag{3}$$

Fig. 3 shows an example of vessel trajectory classification using SRC. 950 training samples are used to generate the training dictionary of SRC, which consists of 18 classes. The test sample can be represented by training samples from different classes. According to the calculations of residuals, the residual from class 2 has the minimum value. Thus, the class of the test trajectory is class 2.

However, solving model (2) has the well-known NP-hard. In order to find solution, many studies often change this nonconvex problem (L0-minimization) into a convex problem (such as L1-minimization and L2-minimization). The L1-minimization problem can be formulated as follows:

$$\min \widehat{A} := ||A||_1$$

$$s.t.||y - DA||_2^2 \le \varepsilon \tag{4}$$

The solution of model (4) can be obtained in polynomial time using second-order core programming or standard linear programming solvers. If the solution of model (4) is sufficiently sparse, the solution can be considered as the solution of model (2) in term of the theories of compressed sensing (Candes and Tao, 2005). However, the solution of model is often insufficiently sparse in practice (Chen et al., 2010).

Similarly, many studies change L0-minimization problem into L2-minimization problem. The model (2) can be transformed as follows:

$$\min \widehat{A} := ||A||_2$$

$$s.t.||y - DA||_2^2 \le \varepsilon \tag{5}$$

Although the solution of model (4) can be found using some heuristic methods, the solution is also far from sparsity in practice.

Recently, some studies find that the sparser solution can be obtained based on Lp-minimization. Thus, l_p-norm regularized problems is applied in this study. The model (2) can be transformed as follow:

$$f(\widehat{A}) := \text{arg min}\{||y - DA||_2^2 + \lambda||A||_p\} \tag{6}$$

To enhance the effectiveness of SRC, a regularization based on Euclidean distance is employed in the SRC model. The model (11) can be rewritten as follows:

$$f(\widehat{A}) := argmin\{||y - DA||_2^2 + \lambda||A||_p + wE(y, DA)\} \tag{7}$$

where w is a regularization coefficient corresponding to $E(y, DA)$ and $E(y, DA)$ is the Euclidean distance between the test trajectory and the selected training dictionary.

As mentioned above, the optimization problem of Lp-minimization is not convex, and convex optimization solvers cannot be applied to solve the sparse representation models. To this end, a Matching Pursuit - Fletcher Reeves (MPFR) algorithm is developed to obtain the solution of model (12).

Algorithm 1: MPFR

Input: training dictionary D, test sample y, threshold ε, the stopping criterion $\|R_0\| < \varepsilon, f, \nabla f$

1. **initialization:** iteration counter q=1, u=0, and set
   - the initial residual R_0=y,
   - the initial solution x_0=0,
   - index $\Gamma_0 = \phi$.
2. **while** stopping criterion has not been met
   1) Find the index j_q according to
   $$j_q = \arg\max_i(\|R_{q-1} \cdot d_i\|_2^2 - wE(y \cdot d_i))$$
   2) Let $\Gamma_q = \Gamma_{q-1} \cup \{j_q\}$
   3) Compute $x_0 = (D_{\Gamma_q}^T D_{\Gamma_q})^{-1} D_{\Gamma_q}^T y$
   4) Calculate the new residual $R_q = y - D_{\Gamma_q} x_0$
   5) q ← q + 1
3. **end while**
4. **compute** $E_0 = -\nabla f(x_0)$
5. **while** $\nabla f(x_u) \ne 0$ **do**
   1) compute α_u by Armijo line search
   2) compute $x_{u+1} = x_u + \alpha_u E_u$
   3) compute $\beta_{u+1}^{FR} = \frac{\nabla f(x_{u+1})^T \nabla f(x_{u+1})}{\nabla f(x_u)^T \nabla f(x_u)}$
   4) $E_{u+1} = -\nabla f(x_{u+1}) + \beta_{u+1}^{FR} E_u$
   5) u ← u + 1
6. **end**

Output: sparse coefficient vector x_u, index Γ_q

Fig. 4 shows the framework of the proposed method. First, vessel motion trajectories are represented by LCSCA, and vessel motion trajectories generate a dictionary of SRC. Then, the dictionary and test trajectory are input into the improved SRC model based on the l_p-norm. In order to find sparse coefficients, a novel method (MPFR) is proposed. Finally, the class of vessel motion trajectory can be classified in term of the minimizing the residual.

3. Experiments and results

To validate the performance and effectiveness of the proposed method, two datasets were used in this study. The vessel trajectories are collected using the AIS base stations, which are installed beside the Yangtze River Bridge in Wuhan and Jiangyin Bridge in Taizhou. The researched areas and sensor devices are shown in Fig. 5.

For the collected AIS data, it is necessary to eliminate data that contain errors or missing parts. Then, 600 trajectories are selected as the dataset. In this study, for the Wuhan dataset, there are 5 classes of vessel motion patterns, from Qingchuange to Huanghelou Port (Class-1, C1), from Qingchuange to Hanyangmen Port (Class-2, C2), from Hanshui River to Container Terminal (Class-3, C3), from Hanshui River to Yangtze River (Class-4, C4), and from upstream to downstream of the Yangtze River (Class-5, C5). For the Taizhou dataset, 5 classes of vessel motion patterns are also defined. Fig. 6 shows all of the motion patterns of sailing in the Yangtze River. General information about the dataset is shown in Table 1.

In this study, all the experiments are conducted in Matlab. The LCSCA method is applied to ensure that the vessel trajectories all have the same dimension. However, the number of control points of LCSCA must be selected because the number of control points is considered as a significant factor affecting classification accuracy. To find the optimized number of control points, the proposed method is conducted under a different number of control points (ranging from 6 to 15 in this study), and the average classification accuracies for each choice are compared and shown in Fig. 7. According to Fig. 7, the choice of 8 control points can achieve the best classification accuracy. Therefore, 8 control points are used to normalize the vessel trajectories in this study.

To test the performance and effectiveness of the proposed method, Support Vector Machine (SVM), k-Nearest Neighbor (kNN), sparse reconstruction classification with l_1-norm (SRC-L1), sparse reconstruction classification with l_2-norm (SRC-L2), and sparse reconstruction classification with l_p-norm (SRC-Lp), are applied and compared.

To measure the performance of the proposed method, True Positive Rate (TPR) and False Positive Rate (FPR) are used. TPR is defined as follows:

$$\mathrm{TPR} = \frac{TP}{TP + FN}$$

where TP is the number of A class of vessel motions correctly classified as A class, and FN is the number of A class of vessel motions wrongly identified as other classes. TPR can illustrate the rate at which the A class of vessel motions are correctly classified. FPR is defined as follows:

$$\mathrm{FPR} = \frac{FP}{FP + TN}$$

where FP represents the number of other classes incorrectly detected as A class and TN is the number of other classes that have been correctly classified as other classes. FPR represents the percentage of members of A class sample detected as belonging to other classes.

Table 2 show the classification accuracy using different classifiers on the Wuhan datasets. According to the classification accuracy results, the proposed method can achieve highest accuracy for each class (91% for C1, 91.6% for C2, 91.9% for C3, 90.5% for C4, and 90.8% for C5). And the proposed method can obtain the best average classification accuracy 91.2%, followed by SRC-Lp at 89.3%, the SRC-L1 at 88.8%, the SRC-L2 at 87.4, the Knn at 87.1%, and the SVM at 86%. In addition, the results of average FPR using six classifies under Wuhan datasets are recorded in Fig. 8. According to the results, we can know that the FPR of our method is lower than the other compared methods. It can indicate that the number of other classes incorrectly identified as detected class using the proposed method is less than it using compared methods.

Table 3 shows the classification accuracy results using SRC-LP, the SRC-L1, the SRC-L2, the Knn, the SVM, and the proposed method on the Wuhan datasets. As can be seen from Table 3, the classification accuracy of each class show the proposed method is better than the compared methods. According to the average classification accuracy of each class, the best one is obtained by the proposed method (89.8%), and the worst is by SVM (83.9%). For further analysis, the average FPR results are shown in Fig. 9. The results shown in Fig. 9 illustrate that the proposed method achieves better performance compared with the other methods. Therefore, we can know that the proposed method outperforms the compared methods.

4. Conclusions

Classification of vessel motion patterns is one of the most important aspects of analyzing AIS data, and it is useful for improving maritime monitoring, ship safety, and management technology. However, manually analyzing such large volumes of data is a prohibitively large workload. Using machine learning methods, vessel motion patterns can be automatically classified. However, labeling vessel trajectories from the AIS dataset is also a prohibitive workload due to the large amounts of data. Furthermore, the AIS dataset is often missing or incomplete. Thus, these classification methods (such as HMM and SVM) that need a large number of complete training samples to finish classification model may not achieve a satisfactory performance to classify vessel motion patterns. In this study, an improved SRC model based on Lp-norm is proposed to classify vessel motion patterns. In addition, the distance between the test samples and the training samples is used to improve the sparse representation classification model. In order to find the solution of the proposed method, a novel method, Matching Pursuit - Fletcher Reeves (MPFR), is proposed. To validate the performance of the proposed method, the AIS datasets from Yangtze River (Wuhan and Taizhou) are used in our experiment. The results show that the classification accuracies of the proposed method are superior to the representative classification methods, including Support Vector Machine (SVM), k-Nearest Neighbor (kNN), sparse reconstruction classification with l_1-norm (SRC-L1), sparse reconstruction classification with l_p-norm (SRC-Lp) and sparse reconstruction classification with l_2-norm (SRC-L2). Future work will study using online classification methods to classify vessel motion patterns.

Acknowledgment

This work was supported in part by the National Natural Science Foundation of China under Grants 61703319, 51775396, U1764262; by the Fundamental Research Funds for the Central Universities under Grant WUT: 2018IVB077.

Appendix A

In the LCSCA technique, the knot point τ and trajectory parameter vectors $l = (0, l_2, \cdots l_{N-1}, l_N)$ are defined as follows:

$$\tau = \left\{ \underbrace{0 \quad 0 \quad 0 \quad 0}_{1\cdots 4}, \underbrace{\frac{1}{p-3}, \frac{2}{p-3}, \frac{3}{p-3}, \cdots, \frac{p-4}{p-3}}_{5\cdots p}, \underbrace{1 \quad 1 \quad 1 \quad 1}_{p+1\cdots p+4} \right\}$$

$$l_t = \frac{h_t}{h_n} = \frac{\sum_{i=2}^{t}\sqrt{(x_i - x_{i-1})^2 + (y_i - y_{i-1})^2}}{\sum_{i=2}^{N}\sqrt{(x_i - x_{i-1})^2 + (y_i - y_{i-1})^2}} \qquad (t = 2, 3, \cdots n.\ l_t \in (0, 1])$$

where $\sum_{i=2}^{t}\sqrt{(x_i - x_{i-1})^2 + (y_i - y_{i-1})^2}$ is the total distance traversed at a given point (x_n, y_n).

The cubic B-spline basis function is calculated with the following recursive formulation based on the De-Boor algorithm (De Boor et al., 1978).

$$K_{i,1}(l_t) = \begin{cases} 1 & if\ \tau_i < l_t < \tau_{i+1} \\ 0 & otherwise \end{cases}$$

$$K_{i,j} = \frac{l_t - \tau_i}{\tau_{i+j-1} - \tau_i}K_{i,j} + \frac{\tau_{i+j} - l_t}{\tau_{i+j} - \tau_{i+1}}K_{i+1,j-1}$$

where τ_i is the ith knot of abovementioned τ vector and j is the order of the function.

The control points can be obtained according to Equation (5), and j is chosen to be 4 for cubic splines. Thus,

$$C^{XY} = \varnothing^{\nabla}T^{XY}$$

where $\phi = \begin{Bmatrix} K_{1,4}(l_1) & \cdots & K_{P,4}(l_1) \\ \vdots & \ddots & \vdots \\ K_{1,4}(l_N) & \cdots & K_{P,4}(l_N) \end{Bmatrix}$ and $\varnothing^{\nabla} = (\varnothing^T\varnothing)^{-1}\varnothing^T$.

References

Ahmadi, P., Tabandeh, M., Gholampour, I., 2016. Abnormal event detection and localisation in traffic videos based on group sparse topical coding. IET Image Process. 10 (3), 235–246.

Amaldi, E., Kann, V., 1998. On the approximability of minimizing nonzero variables or unsatisfied relations in linear systems. Theor. Comput. Sci. 209 (1–2), 237–260.

Bennewitz, M., 2005. Learning motion patterns of people for compliant robot motion. Int. J. Robotics Res. 24 (24), 31–48.

Calinon, S., Guenter, F., Billard, A., 2007. On learning, representing, and generalizing a task in a humanoid robot. IEEE Trans. Syst. Man Cybern. Part B 37 (2), 286–298.

Candes, E.J., Tao, T., 2005. Decoding by linear programming. IEEE Trans. Inf. Theory 51 (12), 4203–4215.

Chartrand, R., 2007. Nonconvex regularization for shape preservation. In: IEEE International Conference on Image Processing, vol. 1. IEEE, pp. I–293.

Chartrand, R., 2007. Exact reconstruction of sparse signals via nonconvex minimization. IEEE Signal Process. Lett. 14 (10), 707–710.

Chen, X., Xu, F., Ye, Y., 2010. Lower bound theory of nonzero entries in solutions of l_2-l_p minimization. SIAM J. Sci. Comput. 32 (5), 2832–2852.

Chen, Z., Wang, L., Yung, N.H., 2011. Adaptive human motion analysis and prediction. Pattern Recognit. 44 (12), 2902–2914.

Chen, Z.J., Wu, C.Z., Zhang, Y.S., Huang, Z., Jiang, J.F., Lyu, N.C., Ran, B., 2017. Vehicle behavior learning via sparse reconstruction with l_2-l_p minimization and trajectory similarity. IEEE Trans. Intelligent Transp. Syst. 18 (2), 236–247.

Cheng, H., Dai, Z., Liu, Z., Zhao, Y., 2016. An image-to-class dynamic time warping approach for both 3D static and trajectory hand gesture recognition. Pattern Recognit. 55, 137–147.

De Boor, C., De Boor, C., Mathématicien, E.U., De Boor, C., De Boor, C., 1978. A Practical Guide to Splines, vol. 27. Springer-Verlag, New York, p. 325.

Fan, J., Li, R., 2001. Variable selection via nonconcave penalized likelihood and its oracle properties. J. Am. Stat. Assoc. 96 (456), 1348–1360.

Field, M., Stirling, D., Pan, Z., Ros, M., Naghdy, F., 2015. Recognizing human motions through mixture modeling of inertial data. Pattern Recognit. 48 (8), 2394–2406.

Hu, W., Tian, G., Li, X., Maybank, S., 2013. An improved hierarchical dirichlet process-hidden markov model and its application to trajectory modeling and retrieval. Int. J. Comput. Vis. 105 (3), 246–268.

International Maritime Organization, 2003, January 6. Guidelines for the Installation of a Shipborne automatic Identification System (AIS). Retrieved July 16, 2017, from. http://www.imo.org/en/OurWork/Safety/Navigation/Documents/227.

Li, C., Han, Z., Ye, Q., Jiao, J., 2011. Abnormal behavior detection via sparse reconstruction analysis of trajectory. In: Sixth International Conference on Image and Graphics. IEEE Computer Society, pp. 807–810.

Liao, L., Fox, D., Kautz, H., 2007. Hierarchical conditional random fields for GPS-based activity recognition. In: Robotics Research: Results of the, International Symposium, Isrr 2005, October 12-15, 2005, San Francisco, Ca, USA, vol. 28, pp. 487–506. DBLP.

Moldenhauer, J., Boesnach, I., Beth, T., Wank, V., Bos, K., 2006. Analysis of human motion for humanoid robots. In: IEEE International Conference on Robotics and Automation. IEEE, pp. 311–316.

Nikolova, M., 2005. Analysis of the recovery of edges in images and signals by minimizing nonconvex regularized least-squares. Multiscale Model. Simul. 4 (3), 960–991.

Psarrou, A., Gong, S., Walter, M., 2002. Recognition of human gestures and behaviour based on motion trajectories. Image & Vis. Comput. 20 (5), 349–358.

Santos, L., Khoshhal, K., Dias, J., 2015. Trajectory-based human action segmentation. Pattern Recognit. 48 (2), 568–579.

Sillito, R.R., Fisher, R.B., 2010. Semi-supervised learning for anomalous trajectory detection. In: British Machine Vision Conference 2008, September, Leeds, UK, vol. 1. DBLP, pp. 1035–1044.

Sun, S., Zhao, J., Gao, Q., 2015. Modeling and recognizing human trajectories with beta process hidden Markov models. Pattern Recognit. 48 (8), 2407–2417.

Wright, J., Yang, A.Y., Ganesh, A., Sastry, S.S., Ma, Y., 2009. Robust face recognition via sparse representation. IEEE Trans. Pattern Anal. Mach. Intell. 31 (2), 210–227.

Yang, M.H., Ahuja, N., Tabb, M., 2002. Extraction of 2d motion trajectories and its application to hand gesture recognition. IEEE Trans. Pattern Anal. Mach. Intell. 24 (8), 1061–1074.

Yu, Y., Barner, K., 2008. Hybrid feature selection for gesture recognition using support vector machines. In: IEEE International Conference on Acoustics, Speech and Signal Processing. IEEE, pp. 1941–1944.